1 **Response to reviewer's second comments on "Summertime episodic chlorophyll-a blooms**
2 **near the east coast of Korea" by Y. -T. Son, J. -H. Park, and S. H. Nam**

3 The authors would like to thank the editor and reviewer for careful and constructive comments.
4 We have responded to the reviewer's comments (written in black) as below in blue.

5 _____

6 Reviewer #1

7

8 Review of: Summer-time episodic chlorophyll-a blooms near east coast of Korea
9 by Young-Tae Son, Jae-Hyoung Park, and SungHyun Nam
10
11 Manuscript ID: BG 2018 183 (2nd submission)
12
13 General comments
14
15 This paper has greatly improved and I thank the Authors for the effort.
16

17 I suggest some minor revisions below, after which I deem the paper to be ready for publication. Details
18 can be found below, and the Authors can contact me via the Editor, anytime for any questions. I do have
19 a scientific question for the Authors, NOT part of the review, but maybe for future work, if they want.
20 If you compare salinity in Fig. 6 with the rest, you find out that the summer 2012 at ESROB is way
21 more saltier. Are the authors planning to find out why? Also, in general, the salinity drops in summer
22 but not always in the same way. E.g. mid-June to mid-August in 2011 (Fig. 5), then there is NO DROP
23 in 2012 (Fig. 6) and from mid-July to end of record beyond September in 2013 (Fig. 7). Why this
24 variability in salinity drop period? And also why this salinity drop at all? From the figures it doesn't
25 look as if it's due to rainfall. Anyway this is just a curiosity.

26 Thank you for the questions and interest. We appreciate the reviewer's constructive comments. There
27 are surely interesting features observed at ESROB and not detailed as a focus in this paper, which
28 include the interannual variation in the summer-mean alongshore current and water properties such as
29 salinity near the coast. Yes, the salinity variations are hardly explained solely by the local precipitation
30 (rainfall) minus evaporation. We are currently analyzing the long-term (~16 years) time-series data
31 collected at ESROB, and more than happy to discuss the results with this reviewer, beyond this paper.
32 Our preliminary results suggest that the equatorward propagating coastal-trapped waves (CTWs),
33 forced primarily by remote winds off the Russian coast, along with influence of cross-shore movement
34 of the poleward-flowing offshore current (EKWC), play a decisive role in the interannual anomalies of
35 the alongshore current.

36

37 The English of the manuscript is now correct, with a few little additional corrections (see below).
38 Particular comments and suggested text corrections
39

40 Title, Abstract and 1. Introduction
41 OK.
42

2 Data and Methods

Line 62. "upper-most" -> "uppermost"
We have revised the word following the suggestion.

Line 86. "at a position 50 times higher than previous polar orbiting ocean color satellites" -> "and its altitude is 50 times higher (35,786 km) than that of polar orbiting ocean color satellites". GOCI is not polar orbiting because it's goo-stationary, so non need for "previous", I guess.
We have revised the phrase following the suggestion.

Line 90. "applying" -> "by applying"
We have revised the word following the suggestion.

Line 95. "variation for spatial Chl a distribution" -> "variation in Chl a spatial distribution"
We have revised the phrase following the suggestion.

Line 98. "by Korea" -> "by the Korea"
We have revised the word following the suggestion.

3. Results
3.1. Climatological CF variations

Lines 21-22 and Fig. 3. "Weak poleward... prevailed". From Fig. 3, how do you explain that, in Jan-May and Oct-Dec, alongshore currents are poleward (weakly positive) when alongshore wind stress is equatorward (negative)? Is the current not wind-driven in these months? (This is not mandatory, but interesting to have a comment).
It is reported from Park et al. (2016) that an equatorward reversal of coastal current in summer opposes poleward local wind stress and offshore current (EKWC). They suggest, by analyzing long time-series data collected at ESROB and other supplementary data, that the alongshore buoyancy gradient driven by the wind curl gradient and the prevalence of warmer and lower salinity water of northern origin balances the lateral friction.

3.2. CF events observed in summers of 2011, 2012, and 2013

Line 125-6. "where the surface CF was significantly" -> "by the surface CF being significantly".
We have revised the phrase following the suggestion.

Line 126-7. "were defined as a period of" -> "were defined as the period during which"
We have revised the phrase following the suggestion.

Line 146. "(showing downwelling induced by equatorward wind stress)" -> "(a consequence of downwelling induced by the equatorward wind stress, as also testified by the rise in temperature at all levels before e04, in Fig. 6 d)". I wrote "the rise in T", but if you have a better idea for proof, please write it in its place. That is, I think you should (easily) prove with your data that you have downwelling, because the equatorward the current is not a definite proof, though it goes in the good direction.

88   We have confirmed the temperature increase and revised the phrase following the suggestion.

89
90   3.3. Surface CF distributions
91
92   Line 175. "reached to JJ" -> "reached JJ"
93   We have revised the word following the suggestion.

94
95   Line 175. "farther south near the coast by July 27" -> "most probably hit ESROB by July 27 (Fig. 8d is
96   cloudy, but salinity drops in Fig. 7)"
97   We have revised the phrase following the suggestion.

98
99   Line 179. "Interestingly" -> "Coherently with this picture,"
100   We have revised the word following the suggestion.

101
102   Line 183. "main axis" -> "its main axis"
103   We have revised the word following the suggestion.

104
105   Line 189. "The offshore advection of coastal plume water of northern origin..." For the E10 event, Fig.
106   7 shows near-zero currents at ESROB. Also, salinity doesn't show a wedge drop. Also, Fig. 9c shows a
107   cyclonic eddy offshore of SO-BGN-DH. So how can one be sure that E10 is not due to recirculation of
108   southern CF-rich water? I think it could be either or both northern OR southern CF-rich water. Chl
109   imagery would solve the problem, but is not available, buit the lack of a wedge drop in SSS is maybe a
110   telltale that it is an E07-like event (even though summer salinity is in general much lower than that at
111   E07).
112   We agree that E10 'may' be affected by the CF-rich water of either or both northern and southern origins.
113   Although we do not rule out the possibility the reviewer suggested with no available GOCI CF image,
114   we retain the description (retaining 'may') raising the other possibility based on 1) equatorward
115   advection of the coastal plume water or northern origin having low salinity, high temperature, and high
116   CF (Fig. 7), and 2) dominant offshore current near DH and ESROB (Fig. 9c).

117
118   Discussion
119
120   4.1. Horizontal advection
121
122   Line 197. "8 of 10" -> "8 out of 10"
123   We have revised the word following the suggestion.

124
125   Line 215. "transportation" -> "transport"
126   We have revised the word following the suggestion.

127
128   Line 224. "half the" -> "half of the"
129   We have revised the word following the suggestion.

130
131   Lne 226 -> "northern origin" -> "northern origin, similarly to E09 and other northern water advection

132 events," (just to give a little more coherence among the "classes" of events you talk about, i.e. northern
133 vs. southern water advection events).
134 We have revised the phrase following the suggestion.

135
136 4.2. Other mechanisms
137
138 Line 244. "nutrient supplied" -> "nutrients supplied"
139 We have revised the word following the suggestion.

140
141 Line 245. "by surface" -> "by the surface"
142 We have revised the word following the suggestion.

143
144 Line 251. "averaged" -> "average"
145 We have revised the word following the suggestion.

146
147 4.3. Inter-annual variations
148
149 Line 267. "in and around" -> "to and around"
150 We have revised the word following the suggestion.

151
152 Line 268. "year-to-year" -> "from year to year" (maybe better)
153 We have revised the word following the suggestion.

154
155 Line 273. "half the" -> "half of the"
156 We have revised the word following the suggestion.

157
158 Line 277. "coastal trapped" -> "coastally trapped"
159 We have retained the original word as widely used by the community.

160
161 Line 285. "impact of EKWC" -> "role of the EKWC"
162 We have revised the word following the suggestion.

163
164 Line 286. "yields less" -> "reveals a reduced"
165 We have revised the word following the suggestion.

166
167 Line 286. "in 2011" -> "during the 2011"
168 We have revised the word following the suggestion.

169
170 Line 287. "than 2012" -> "than in the 2012"
171 We have revised the word following the suggestion.

172
173

174   5. Concluding remarks

175

176   Line 293. "northern coast" -> "northern Korean coast"

177   We have revised the word following the suggestion.

178

179   Line 301. "play" -> "plays"

180   We have revised the word following the suggestion.

181

182   Tables, Figures and captions

183

184   Line 404. Figure 1 caption. "rainfall station" -> "rainfall stations"

185   We have revised the word following the suggestion.

186

187   Line 413. Figure 2 caption. "(dash lines)" -> "(dashed lines)"

188   We have revised the word following the suggestion.

189

190   Figure 3. The labels in the rectangles of each panel (E.g. WSa, WSc in the top plot) are virtually

191   unreadable, especially subscripts, also at a 120% zoom, please enlarge characters. Lines are OK.

192   The characters in the labels have been enlarged.

193

194   Line 423. Figure 4 caption. "percentage saturation" -> "percent saturation"

195   We have revised the word following the suggestion.

196

197   Line 479. Figure 10 caption. "colorbar in the right" -> "colorbar on the right".

198   We have revised the word following the suggestion.

199

200

Summertime episodic chlorophyll-a blooms near the east coast of Korea

Young-Tae Son, Jae-Hyoung Park, and SungHyun Nam[*]

School of the Earth and Environmental Sciences/Research Institute of Oceanography, Seoul National University, Seoul 08826, Republic of Korea

[*]Correspondence to namsh@snu.ac.krnamsh@snu.ac.kr

212 **Abstract**. We present intensive observational data of surface chlorophyll-a bloom episodes occurring
213 over several days in the summers of 2011, 2012, and 2013, accompanying the equatorward advection
214 of low sea-surface salinity (SSS) water near the east coast of Korea. Time-series analysis of
215 meteorological and oceanographic (physical and biochemical) parameter data, such as chlorophyll
216 fluorescence (CF) from surface mooring, ocean color (chlorophyll a and total suspended sediment), sea
217 surface height (satellite-derived), and serial hydrographic data (from in-situ measurements) were used
218 to investigate the relationship between surface bloom events and changes in seawater characteristics
219 and currents. In the summers of the three years, a total of 10 bloom events (E01–E10) were identified
220 where the surface CF was significantly (> 2 μg/l) enhanced over a relatively long (> 1 d) period. The
221 bloom events in the summers of 2011 and 2012 were accompanied by low or decreasing SSS for several
222 days to a week after heavy rainfall at upstream stations and equatorward currents. Unlike the typical 8
223 of the 10 events (80 %), E07 was potentially derived from the onshore advection of high CF offshore
224 water of southern origin into the coastal zone near the mooring, whereas E10 possibly prevailed by
225 offshore advection of high CF plume water trapped by the coastal area. Contrasting with many coastal
226 systems, these findings indicate that event-scale productivity near the east coast of Korea in summer is
227 not controlled by local blooms triggered by either nutrients or light availability, but by the equatorward
228 and cross-shore advections of high CF plume water.

229

1. Introduction

Biological blooms associated with, among other phenomena, the horizontal advection of chlorophyll-rich water (often having low-salinity and high nutrients linked to heavy rain, e.g., nutrient loading), have been frequently observed in many coastal systems (e.g., Yin et al., 2004; Dai et al., 2008; Halverson and Pawlowicz, 2013; Reifel et al., 2013). Blooms stimulated by plume-delivered nutrients and enhanced stratification were observed near and offshore of Hong Kong (Dai et al., 2008; Yin et al., 2004). During bloom events, a several-fold increase in chlorophyll a (Chl a) and significant shift in phytoplankton community structure were observed (Dai et al., 2008). The effects of effluent discharge plumes on coastal phytoplankton communities were examined from the City of Los Angeles Hyperion Wastewater Treatment Plant, demonstrating that localized blooms occurred a few days after the plume water discharge (Reifel et al., 2013). The Fraser River plume affects Chl a distribution in the Strait of Georgia, British Columbia, Canada, revealing large Chl a differences among the local plumes, despite insensitivity in the long-term average (Halverson and Pawlowicz, 2013).

There are several small river plumes potentially affecting Chl a distribution near and offshore of the east coast of Korea; yet, the effects remain poorly understood. High summer (from June to September, JJAS) precipitation often accompanying heavy rainfall around the Korean peninsula accounts for >50% of the annual precipitation in the region. During summer, most rivers in the region become flooded and discharge large volumes of freshwater into the adjacent marginal seas, including the East Sea (Japan Sea), Yellow Sea, and East China Sea (Bae et al., 2008; Kong et al., 2013). Chl a distribution in the southwestern East Sea off the east coast of Korea has been found to be associated with physical processes at mesoscale or larger scales, including spring and fall blooms that have been detected using satellite ocean color data, data from short-duration ship surveys (Hyun et al., 2008; Kang et al., 2004), and time-series data collected continuously from moored buoys (Hong et al., 2013; Son et al., 2014). Despite wide range images available from geostationary and polar-orbit satellite ocean color remote sensing (Yoo and Kim, 2004; Son et al., 2014; Hyun et al., 2008; Kim et al., 2011), phytoplankton blooms observed over several days to weeks near the coast, particularly during the well-stratified summer season, have rarely been examined. Thus, we aimed to address the episodic bloom events in summer and investigated the effects of river plumes on Chl a distribution near and away from the east coast of Korea.

2. Data and methods

Time-series data of meteorological, physical, and biochemical parameters have been measured using a surface mooring named ESROB (East Sea Real-time monitoring Ocean Buoy), deployed in a water depth of 130 m, about 8 km off the mid-east coast of Korea (Fig. 1). The collected data included wind speed and direction at 2 m above the sea surface, photosynthetically active radiation (PAR) at about 2 m above the sea surface and at a depth of 10 m , temperature and salinity at five depths (5, 20, 40, 60, and 110 m), current vertical profiles with an interval (bin size) of 4 m (upper mostuppermost bin corresponds to 5 m depth), and sea surface temperature (SST), salinity (SSS), dissolved oxygen (DO), and chlorophyll fluorescence (CF) measured by a Water Quality Monitor (WQM) at a depth of about 1 m. Details on the technical design, improvements, and early-phase operations of ESROB

266 have been previously described (Nam et al., 2005). In the present study, we used data collected for ~3 years, from
267 April 2011 to December 2013, with an emphasis on the three summer periods (JJAS) when the poleward
268 alongshore current (showing a general width of up to about 40 km) averaged over 6 years reversed to an
269 equatorward direction (Park et al., 2016).

270 The CF as a factory-calibrated Chl a concentration in units of µg/l following the manufacturer's (WET Lab)
271 instructions always needs calibration with in-situ measurements owing to long-term sensor drift and that different
272 Chl a concentrations may yield the same fluorescence energy (Longhurst et al., 1989). Four cruises were
273 conducted in July and October 2011, April 2012, and July 2013 to collect in-situ water samples for Chl a and in-
274 situ sensor measurements for water temperature and salinity near the coast. A statistically significant correlation
275 (r^2 = 0.76, p < 0.001) was found between the CF sensor values and in-situ chlorophyll concentration derived from
276 the spectrophotometer using acetone-extracted Chl a (Fig. 2a). In addition to the chlorophyll calibration, the
277 concentrations of nitrate were analyzed simultaneously with 64 samples to determine the nitrate proxy based on
278 the relationship between temperature and nitrate. Separately, to observe the fine-scale coastal SST and SSS
279 distributions around the ESROB, in-situ measurements using a small research vessel equipped with a
280 thermosalinograph (SEB21, 10 s sampling interval) were conducted on July 30, 2013, a couple of days after heavy
281 rainfall. Since non-photochemical quenching (NPQ) has a significant influence on the CF in response to changes
282 in ambient light (Müller et al., 2001), particularly for a single channel excitation Chl a fluorometer, the effects
283 were corrected from the ESROB CF data following the methods described in Halverson and Pawlowicz (2013)
284 before calibrating with in-situ water samples.

285 We used high-resolution daily data generated by the geostationary ocean color imager (GOCI) satellite
286 (composited using eight images) to estimate surface Chl a distributions. The spatial resolution of the GOCI is 500
287 m ~~at a position~~and its altitude is 50 times higher (35,786 km) than ~~previous~~that of polar orbiting ocean color
288 satellites (Ryu et al., 2012). Chl a concentration observed from the GOCI can be easily contaminated by total
289 suspended sediment (TSS) and colored dissolved organic matter (CDOM) in the coastal regions (Ryu et al., 2012).
290 Thus, the GOCI Chl a was calculated through software modules of the GOCI Data Processing System (GDPS,
291 described in Han et al., 2010 and Ryu et al., 2012) by applying a correction algorithm for the TSS and CDOM, as
292 well as by minimizing the contaminating effects of cloud, sea fog, and aerosols (level 1B). Nevertheless,
293 relationships between the GOCI Chl a and TSS in coastal and offshore areas in Fig. 1 were compared with a linear
294 regression to determine the Chl a in the coastal region (Fig. 2b, c). Results exhibited that the higher the value, the
295 wider the scatter. Despite that the absolute value of Chl a can be overestimated at high TSS (Kim et al., 2016),
296 this indicates that the GOCI Chl a in this area is still useful for understanding the variation ~~for~~in Chl a spatial ~~Chl~~
297 ~~a~~ distribution because the horizontal pattern of Chl a is realistic. Satellite altimeter-derived sea surface height
298 (SSH) products corrected using coastal tide-gauge sea level data along the east coast of Korea (Choi et al., 2012)
299 were used to examine surface geostrophic currents around and offshore of the ESROB in the summer of 2013.
300 Precipitation data (provided by the Korea Meteorological Administration (KMA)) were also used to compare the
301 bloom timings with those of heavy rainfall in summer. Precipitation (mm/day) was recorded every 3 h during the
302 summers of 2011, 2012, and 2013 at stations along the coast (SP: SinPho, HH: HamHeung, WS: WonSan, JJ:
303 JangJun, SO: Sockcho, BGN: BukGangNeung, DH: DongHae), and the data were proxied as freshwater

304 discharges from several small rivers into the East Sea (Fig. 1) without available data for freshwater discharges
305 along the North Korean coast.

306 Current and wind vectors were corrected for local magnetic deviation, decomposed into alongshore and cross-
307 shore components rotating counter-clockwise from the north by 30 °. Wind stresses have been calculated following
308 $\vec{\tau} = \rho_a C_D |W| \vec{W}$ (ρ_a: air density, C_D: drag coefficient, $\vec{W}$: wind), and alongshore and cross-shore components
309 of current (V_a and U_c) and wind stress (WS_a and WS_c) are expressed by the coordinate transformation, respectively
310 (Large and Pond, 1981). All variables were low-pass filtered with the half power centered at 40 h.

311

3. Results

3.1. Climatological CF variations

314 Annual cycles of wind stress (WS_a, WS_c), surface CF, SST, SSS, surface DO, and surface current ((V_a, U_c) at the
315 ~~upper most~~uppermost bin) observed at ESROB were obtained by climatologically averaging monthly mean values
316 over the three years from 2011 to 2013, which showed significant summertime CF enhancements (in addition to
317 two well-documented blooms in spring and fall), weakened wind forcing, increased SST, decreased SSS, over-
318 saturated surface DO (though absolute DO decreased), and strengthened equatorward ($V_a < 0$) surface currents
319 (Fig. 3). The CF enhancements during the summer with significantly high concentrations > 1 µg/l in July
320 accompanied by decreased SSS (abruptly decreased from June to July) and strengthened equatorward currents
321 (maximum speed of 15 cm/s in July), implied high Chl a and low salinity water of northern origin. Although
322 absolute DO decreased with increasing SST, the surface water was over-saturated for most of the summer,
323 implying a significant role of surface bioactivity. Weak poleward ($V_a > 0$ and $U_a \sim 0$) surface currents were
324 observed throughout the year, except in summer, when strong equatorward ($V_a < 0$ and $U_a \sim 0$) currents prevailed~~.~~
325 (Park et al., 2016).

326

3.2. CF events observed in summers of 2011, 2012, and 2013

328 In the summers of 2011, 2012, and 2013, 10 bloom events (E01–E10) were identified ~~whereby~~by the surface CF
329 ~~was~~being significantly enhanced over a considerable period, i.e., days to weeks (Fig. 4, Table 1). The CF bloom
330 events were defined as ~~a~~the period ~~of~~during which CF > 1.0 µg/l basically. Then, among the events, we selected
331 only those where the duration of CF > 2.0 µg/l was longer than 1 d as the final events. The summer bloom event
332 lasted for several days to weeks, which is shorter than the typical duration of spring and fall blooms. Six events,
333 three in each year (E01–E03 and E04–E06), were identified in the summers of 2011 and 2012, whereas four (E07–
334 E10) occurred in 2013 (Fig. 4). The average SST, SSS, and CF for the duration of each event are listed in Table 1.

335 During the CF events in the summer of 2011 (E01–E03), low SSS was observed at ESROB several days to a week
336 after remarkable wind forcing and heavy rainfall (maximum of 160 mm/day during E02) at upstream stations,
337 accompanying enhanced equatorward currents (Fig. 5a, c, e, and f). Two typhoons (MAON and MUIFA) yielding
338 a maximum wind stress of 0.25 N/m^2 passed through the region during the CF bloom events, inducing strong

339   equatorward (before E01) and poleward (after E03) wind stresses (arrows labeled by M1 and M2 in Fig. 5b) and

340   implying downwelling (before E01) and upwelling (after E03) in the vicinity of ESROB. Interestingly, the

341   equatorward (poleward) wind stress may strengthen equatorward (poleward) and onshore (offshore) surface

342   currents. Indeed, strong equatorward currents were observed up to 2 d after the peak wind forcing immediately

343   before E01, whereas the equatorward currents were markedly weakened by the poleward wind stress immediately

344   after E03 (Fig. 5b, f).

345   Similarly, the CF events in the summer of 2012 were also accompanied by low or decreasing SSS several days to

346   a week after heavy rainfall at upstream stations and equatorward currents (Fig. 6a, c, e, and f). Three (KHANUN,

347   BOLAVEN, and TENBIIN) among the four typhoons in the summer affected the surface CF, SSS, and surface

348   currents during the events. Since typhoon KHANUN drove poleward wind stress, the strong equatorward currents

349   (~~showing~~a consequence of downwelling induced by the equatorward wind stress, as also testified by the rise in

350   temperature at all levels before E04, Fig. 6d) developed before and during the most of E04 were weakened, and

351   SSS increased to reduce the salinity stratification and decrease surface CF during E04 (arrow labeled by K in Fig.

352   6b, c, e, and f). After the typhoon passed, the surface CF increased again along with re-enhancing equatorward

353   currents, re-stratifying salinity, and decreasing SSS during E05 (Fig. 6c, e, and f). Two typhoons (BOLAVEN and

354   TENBIIN) successively passed the area and poleward (equatorward) wind stress imposed by BOLAVEN

355   (TENBIIN) induced an upwelling (downwelling) response with poleward (equatorward) and offshore (onshore)

356   transports at the upper layer, decreasing (increasing) water temperature, and increasing (decreasing) salinity in the

357   whole column during E06. The poleward wind stress imposed by the BOLAVEN induced well-mixed conditions

358   with high SSS, low SST, and strong poleward surface currents (arrow labeled by B in Fig. 6b, c, d, and f). However,

359   the reversed wind stress imposed by the successive TENBIN resulted in decreasing SSS, increasing SST,

360   weakening the poleward surface current (strengthening equatorward surface current), and rapidly increasing

361   surface CF (peak exceeding 4.5 µg/l) (arrow labeled by T in Fig. 6b, c, d, e, and f).

362   Contrasting to the CF bloom events in the summers of 2011 and 2012, two among the four events (E07 and E10)

363   in the summer of 2013 did not follow heavy enough rainfall at the upstream stations nor equatorward currents

364   (Fig. 7a, f). Typical heavy rainfall and enhanced equatorward surface currents preceded low SSS and high surface

365   CF during the other two events (E08 and E09) only (Fig. 7a, f). Unlikely with typical events, the SSS remained

366   high and SST temporally decreased (negative anomaly) during E07 (Fig. 7c and d), whereas relatively high SST

367   and low SSS were observed during E10 (Fig. 7c, d). Contrasting with the other two years, winds were mild, and

368   no typhoon passage was reported in the summer of 2013 (Fig. 7b).

369

370   **3.3. Surface CF distributions**

371   The equatorward advection of low salinity, chlorophyll-rich plume water into the ESROB area along the coast

372   was confirmed from a series of daily composite GOCI Chl a only when clear images containing few clouds were

373   available. One example presented here is from four images continuously available from July 24 to 27, 2013, before

374   E09 (Fig. 8a–d). A high surface CF zone in the northern area (e.g., off the SP, HH, and WS sites, Fig. 1) was

375   separated from that in the southern area (e.g., between the coast and UI, Fig. 1) following the poleward current—

376 the East Korea Warm Current (EKWC)—whereas a more coastal branch extended equatorward with time near the

377 coast (Fig. 8a–d) after the heavy rainfall of July 19–24 (Fig. 7a). The high CF plume water was elongated and

378 reached ~~to~~ JJ by July 24, SO by July 25–26, and ~~farther south near the coast~~most probably hit ESROB by July 27~~,~~

379 (Fig. 8d is cloudy, but salinity drops in Fig. 7), yielding the E09 event from July 28 to August 1 (Table 1, Fig. 7).

380 The SST and SSS observed using the thermosalinograph on July 30, 2013 in the vicinity of ESROB consistently

381 demonstrated wedge-shaped patterns with low SSS and high SST water confined near the coast and reaching

382 farther south passing BGN (Fig. 8e, f), confirming the equatorward advection of low-salinity and high CF surface

383 water along the coast to ESROB. ~~Interestingly~~Coherently with this picture, the satellite-based surface geostrophic

384 currents around and offshore of ESROB (not shown) and the alongshore currents observed at the upper depths of

385 ESROB (e.g., Fig. 7f) were all equatorward during this period.

386 The patterns of surface CF distribution and geostrophic flow field on July 3, 2013 for E07 are shown in Fig. 9a

387 and b, where high CF was found inshore of the poleward flowing EKWC (its main axis is closer to UI than the

388 high CF area) and within the cyclonic circulation around ESROB (area of relatively low SSH). Onshore currents

389 prevailed between BGN and DH, associated with the cyclonic circulation (Fig. 9b), potentially yielding onshore

390 advection of high CF offshore water of southern origin into the coastal zone near ESROB during E07 (Fig. 9d).

391 Similarly, although clear images were not available at that time, the geostrophic flow field on August 21, 2013 for

392 E10 is shown in Fig. 9c, wherein offshore currents were found to prevail near the coastal zone, near DH and

393 ESROB, as well as equatorward currents immediately to the north. The offshore advection of coastal plume water

394 of northern origin presumably having low salinity, high temperature, and high CF (see in Fig. 7, but also other

395 similar events, as in Fig. 1 or Fig. 8) may have enhanced the surface CF at ESROB during E10 (Fig. 9e).

396

4. Discussion

4.1. Horizontal advection

399 The low-salinity chlorophyll-rich water originating from the northern coastal region often accompanying heavy

400 rainfall is advected equatorward along the coast into the coastal zone in the vicinity of ESROB in summer, and is

401 primarily responsible for most (80 %, 8 out of 10) of the CF events. The rate of Chl a change observed at ESROB

402 is comparable with the rate estimated from the spatial Chl a gradient and speed of equatorward advection. The

403 equatorward advection distance of high Chl a water is measured to be dy = 100 km over 3 d (= dt) with Chl a

404 change (difference between Chl a at the plume source and the initially oligotrophic water at ESROB) of about 2.5

405 μg/l (= dChl) from the series of four daily composites of GOCI Chl a collected in July 24 to 27, 2013 before E09

406 (Fig. 8a–d). With an advective speed of 0.4 m/s (= 100 km / 3 d), this yields a rate of Chl a change of 0.86 μg/l/d

407 (= 0.4 m/s × 2.5 μg/l / 100 km) owing to the alongshore advection ($v\partial$Chl $a/\partial y$), which is consistent with the

408 observed rate (∂Chl $a/\partial t$ where dChl was estimated from the ESROB measurements and dt = 1 h) for E09 (up

409 to 1.26 μg/l/d averaged over the period when ∂Chl $a/\partial t > 0$) and others (mean: 0.87 μg/l/d), supporting that the

410 alongshore advection plays a primary role in CF variability near the coast. The distribution and temporal evolution

411 of SSS observed in July 30, 2013 implies the low salinity plume water (SSS < 29 g/kg found in the northern

412 coastal area, Fig. 8e) is mixed with saline offshore water while advected equatorward, yielding slightly higher (>

413   31 g/kg) SSS at ESROB. These findings are similar to those of bloom events with a rate of CF change (2–4 μg/l/d

414   estimated from their Fig. 11) controlled by the advection of low SSS and high CF plume water in other coastal

415   systems (Halverson and Pawlowicz, 2013).

416   In contrast to E09, the high surface CF observed during E07 is not explained by equatorward advection of low-

417   salinity chlorophyll-rich water originating from the northern coastal region, but potentially by the onshore

418   advection of high CF water of southern origin advected via the EKWC. Hyun et al. (2009) demonstrated that the

419   highest primary productivity in the southwestern East Sea is induced by the ~~transportation~~transport of high CF

420   water originated from upwelling of nutrient rich water along the southern east coast of Korea. The high CF water

421   may affect the productivity near the mid-east coast of Korea as advected by the EKWC and its meanders,

422   particularly on the western or coastal side of the front formed by the EKWC. Indeed, a rate of cross-shore Chl a

423   change around ESROB from the surface CF distribution observed during E07 (Fig. 9a) is roughly 0.1 μg/l/km

424   (dChl = 1.0 μg/l and dx = 10 km) and a rate of Chl a change by cross-shore advection (u $\partial Chl\,a/\partial x$) is estimated

425   to be 0.86 μg/l/d (= 0.1 m/s * 1.0 μg/l / 10 km) with cross-shore velocity of 0.1 m/s (estimated from the ESROB

426   measurements), which supports this assertion, demonstrating the influence of the high CF region offshore on the

427   ESROB site (Fig. 9a, d). Onshore advection of the high CF water originated from the upwelling of nutrient-rich

428   water along the coast, accounts for half of the CF change during the event (up to 1.60 μg/l/d averaged over the

429   E07 when $\partial Chl\,a/\partial t > 0$) observed at ESROB during E07 (Fig. 7). Conversely, offshore advection of high CF

430   coastal plume water of northern origin, similarly to E09 and other northern water advection events, may also be

431   significant, as happens for the E10 bloom. Based on previous research conducted in other coastal systems, E10 is

432   similar to results on temporal and spatial variations of CDOM, CF, and primary productivity by cross-shore

433   (onshore and/or offshore) advection of high SST and high CF plume water associated with local circulations

434   (Brzezinski and Washburn, 2011; Warrick et al., 2007). Thus, cross-shore advection of low SSS and high CF water

435   associated with ambient circulation plays an equally significant role in shaping and triggering bloom events in the

436   coastal area.

439   **4.2. Other mechanisms**

440   The high CF events observed at ESROB are not local blooms triggered by either nutrients or light availability.

441   The upward vertical flux of nitrate into the euphotic zone at Huntington Beach, southern California shows how

442   vertical nutrient supply triggers local chlorophyll blooms (Omand et al., 2012). Omand et al. (2012) demonstrated

443   that each episodic bloom was preceded by a vertical nitrate flux event 6–10 days earlier using nitrate

444   concentrations estimated from a temperature proxy. Relationships between nitrate and temperature and between

445   nitrate and salinity observed from the surveys in July and October of 2011 and April of 2012 are not significantly

446   different from each other, and the vertical nitrate fluxes were estimated by the temperature proxy to discuss the

447   potential role of nitrate in triggering the episodic blooms. However, both advective and turbulent nitrate fluxes

448   estimated using a nitrate proxy utilized from temperature measurements (Fig. 10) did not account for the observed

449   CF blooms (not shown). Moreover, local blooms triggered by ~~nutrient~~nutrients supplied by equatorward advection

450   is not supported by surface CF distribution (decreasing equatorward) in July 24 to 27, 2013 (Fig. 8). Although

451   some episodic CF blooms (E01 and E06) are preceded by flux peaks with a typical time lag of 4–12 d, most events

452   are not directly linked to the variability in vertical nitrate fluxes, suggesting only minor roles of nutrient flux in

453   shaping CF variability observed at ESROB in summer.

454   Time-series of the euphotic zone depth (Z_{eu}) were compared with the other time-series data recorded at ESROB

455   to examine the effects of light adaptation on the bloom events, using the data collected with two PAR sensors

456   available for 2012 and 2013 (Figs. 6, 7). Basically, the ~~averaged~~average for the E04 to E10 bloom periods, Z_{eu} =

457   18 m, was deeper than 10.5 m which is Z_{eu} averaged over the two whole summer periods (JJAS), indicating that

458   the light environment was favorable at least for retaining and increasing of the CF bloom observed at ESROB. A

459   Z_{eu} of 20 m obtained by averaging over the three bloom events (E04–E06) in 2012 was deeper than that (Z_{eu}=15

460   m for E07–E10) in 2013, supporting more favorable CF bloom conditions in 2012 than 2013. Correspondingly,

461   CF of 1.8 µg/l averaged over E04–E06 in 2012 was higher than that in 2013 (~ 1.6 µg/l for E07–E10). Our results

462   on the deeper Z_{eu} with higher CF in 2012 than 2013 summers are consistent with those in other systems (e.g.,

463   Mississippi River coastal system) where light attenuation plays a significant role in increasing phytoplankton

464   biomass, and productivity variation (Lehrter et al., 2009). However, the CF changes among the individual events

465   do not necessarily follow Z_{eu} variations (Table 1), suggesting a minor role of light availability in shaping the CF

466   variability observed at ESROB.

467

4.3. ~~Inter-annual~~Interannual variations

469   The CF bloom events near the coast can vary inter-annually depending on the passage of typhoons. Five typhoons

470   that passed through this area were associated with the CF bloom events for two summers (2011 and 2012) and

471   there was no typhoon affecting the CF bloom events in 2013 summer. Both strong wind forcing and intensive

472   rainfall associated with typhoon passage nearby determine how the plume water is advected ~~into~~ and around

473   ESROB, which varies from year- to- year. In 2011, for example, the CF enhancement (E01) was accompanied by

474   the passage of MAON (equatorward wind stress and current) through the area south of ESROB, whereas E03

475   ended with the passage of MUIFA (poleward wind stress and current) passing through the area north of ESROB

476   (Fig. 5b). Similarly, surface CF decreased (increased) with the passages of typhoons KHANUN and BOLAVEN

477   (TENBIIN) through the area north (south) of ESROB (Fig. 6b). Without any typhoon passage in the summer of

478   2013, only half of the CF events could be explained by the alongshore advection contrasting with those in the

479   other two years (Fig. 7b). Thus, the primary productivity in the area is possibly affected severely by inter-annual

480   variations of typhoon-induced alongshore advection.

481   Remote wind forcing significantly affecting summertime equatorward currents near the coast via equatorward

482   propagating coastal trapped waves (CTWs) varied in the summers of 2011, 2012, and 2013 (Park and Nam, 2018

483   in revision). The CTWs generated off the Russian coast (~1,000 km from ESROB) changed equatorward currents

484   at the location of ESROB to yield more equatorward advection in 2011 and 2012 summers and more poleward

485   advection in 2013 summer, of low-salinity plume water near the coast (Park and Nam, 2018 in revision). These

486   results may be relevant to more CF bloom events explained by equatorward advection of plume water of northern

487 origin in 2011 and 2012 summers than 2013 summer (6 among 6 events vs. 2 among 4 events). Therefore, inter-
488 annual variations of alongshore advection and surface CF blooms near the coast are possibly affected by the CTWs
489 propagating equatorward from the Russian coast, where wind forcing varies considerably to generate CTWs. Park
490 and Nam (2018 in revision) also quantified the ~~impact~~role of the EKWC on the alongshore current variability near
491 the coast, which ~~yields less~~reveals a reduced EKWC impact and more equatorward currents near the coast ~~in~~during
492 the 2011 and 2013 summers, than in the 2012 summer. Although this is inconsistent with less CF bloom events
493 explained by the equatorward advection of plume water of northern origin in 2013 summer, cross-shore advections
494 of high CF water of either northern (E10) or southern origin (E07) are possibly associated with EKWC
495 recirculation based on the patterns of surface geostrophic currents (Fig. 9).

496

497 **5. Concluding remarks**

498 The low-salinity chlorophyll-rich water originating from the northern Korean coast accompanying heavy rainfall
499 is often advected equatorward along the coast in summer, resulting in high surface CF events near the mid-east
500 coast of Korea. Alongshore advection of high CF waters is primarily responsible for most (80 %, 8 of 10) of the
501 CF events, which confirms that the bloom events are possibly controlled by the advection of low SSS and high
502 CF plume water in summer. In contrast to the bloom events associated with alongshore advection, the high surface
503 CF observed during E07 is possibly explained by the onshore advection of high CF water of southern origin
504 advected by the poleward-flowing EKWC. Similarly, offshore advection of high CF coastal plume water of
505 northern origin may be significant, as in the case of E10. Therefore, the equatorward and cross-shore advection
506 of chlorophyll-rich plume water with decreasing SSS ~~play~~plays a primary role in the high productivity near the
507 east coast of Korea in summer. Summertime CF near the coast varies inter-annually as the horizontal advections
508 vary significantly, inter-annually associated with typhoon passages nearby, CTWs generated from the Russian
509 coast, and influence of the EKWC, which should be addressed with long time series data in the future.

510

521

522 **Data availability:** All data are available upon request to the authors.

529 **References**

530 Bae, D. H., Jung, I. W., and Chang, H.: Long-term trend of precipitation and runoff in Korean river basins, Hydro.
531   Proc., 22, 2644–2656, 10.1002/hyp.6861, 2008.

532 Brzezinski, M. A., and Washburn, L.: Phytoplankton primary productivity in the Santa Barbara Channel: Effects
533   of wind-driven upwelling and mesoscale eddies, J. Geophys. Res., 116, 10.1029/2011jc007397, 2011.

534 Choi, B. -J., Byun, D. -S., and Lee, K. -H.: Satellite-altimeter-derived East Sea aurface currents: Estimation,
535   description and variability pattern, The Sea, 17, 225–242, 10.7850/jkso.2012.17.4.225, 2012.

536 Crespo, B. G., Figueiras, F. G., and Groom, S.: Role of across-shelf currents in the dynamics of harmful
537   dinoflagellate blooms in the northwestern Iberian upwelling, Limnol. Oceanogr., 52, 2668–2678, DOI
538   10.4319/lo.2007.52.6.2668, 2007.

539 Dai, M. H., Zhai, W. D., Cai, W. J., Callahan, J., Huang, B. Q., Shang, S. L., Huang, T., Li, X. L., Lu, Z. M., Chen,
540   W. F., and Chen, Z. Z.: Effects of an estuarine plume-associated bloom on the carbonate system in the lower
541   reaches of the Pearl River estuary and the coastal zone of the northern South China Sea, Cont. Shelf Res., 28,
542   1416–1423, 10.1016/j.csr.2007.04.018, 2008.

543 Halverson, M. J., and Pawlowicz, R.: High-resolution observations of chlorophyll-a biomass from an instrumented
544   ferry: Influence of the Fraser River plume from 2003 to 2006, Cont. Shelf Res., 59, 52–64,
545   10.1016/j.csr.2013.04.010, 2013.

546 Han, H. -J., Ryu, J. -H., and Ahn, Y. -H.: Development the Geostationary Ocean Color Imager (GOCI) Data
547   Processing System (GDPS), K. J. Rem. Sens., 26, 239–249, 2010.

548 Hong, G. H., Lee, D. K., Yang, D. B., Kim, Y. I., Park, J. H., and Park, C. H.: Eddy- and wind-sustained moderate
549   primary productivity in the temperate East Sea (Sea of Japan), Biogeosci. Disc., 10, 10429-10458,
550   10.5194/bgd-10-10429–2013, 2013.

551 Hyun, J., Kim, D., Shin, C., Noh, J., Yang, E., Mok, J., Kim, S., Kim, H., and Yoo, S.: Enhanced phytoplankton
552   and bacterioplankton production coupled to coastal upwelling and an anticyclonic eddy in the Ulleung basin,
553   East Sea, Aquat. Microbial Ecol., 54, 45–54, 10.3354/ame01280, 2008.

554 Kang, J. H., Kim, W. S., Chang, K. I., and Noh, J. H.: Distribution of plankton related to the mesoscale physical
555   structure within the surface mixed layer in the southwestern East Sea, Korea, J. Plankton Res., 26, 1515–

556   1528, 10.1093/plankt/fbh140, 2004.

557   Kim, D., Yang, E. J., Kim, K. H., Shin, C. W., Park, J., Yoo, S., and Hyun, J. H.: Impact of an anticyclonic eddy
558   on the summer nutrient and chlorophyll a distributions in the Ulleung Basin, East Sea (Japan Sea), ICES J.
559   Mar. Sci., 69, 23–29, 10.1093/icesjms/fsr178, 2011.

560   Kim, W., Moon, J. -E., Park, Y. -J., and Ishizaka, J.: Evaluation of chlorophyll retrievals from Geostationary
561   Ocean Color Imager (GOCI) for the North-East Asian region, Rem. Sens. Environ., 184, 428–495, 2016.

562   Kong, G. S., Kim, K. -O., and Kim, S. -P.: Characteristics of the East Asian summer monsoon in the South Sea of
563   Korea during the Little Ice Age, Quaternary International, 286, 36-44, 10.1016/j.quaint.2012.07.022, 2013.

564   Large, W. G., and Pond, S.: Open Ocean Momentum Flux Measurement in Moderate to Strong Winds, Journal of
565   Physical Oceanography, 11, 324–336, 1981.

566   Lehrter, J. C., Murrell, M. C., and Kurtz, J. C.: Interactions between freshwater input, light, and phytoplankton
567   dynamics on the Louisiana continental shelf, Cont. Shelf Res., 29, 1861–1872, 10.1016/j.csr.2009.07.001,
568   2009.

569   Longhurt, A. R. and Harrison, W. G.: The biological pump: Profiles of plankton production and consumption in
570   the upper ocean, Prog. Oceanog., 22, 47–123, 1989.

571   Müller, P., Li, X., and Niyogi, K. K.: Non-Photochemical Quenching. A Response to Excess Light Energy, Plant
572   Physiol., 125, 1558–1566, http://doi.org/10.1104/pp.125.4.1558, 2001.

573   Nam, S., Kim, G., Kim, K. -R., and Kim, K.: Application of Real-time Monitoring Buoy Systems for Physical
574   and Biogeochemical Parameters in the Coastal Ocean around the Korean Peninsula, Mar. Technol. Soc. J., 39,
575   70–80, 2005.

576   Omand, M. M., Feddersen, F., Guza, R. T., and Franks, P. J. S.: Episodic vertical nutrient fluxes and nearshore
577   phytoplankton   blooms   in   Southern   California,   Limnol.   Oceanogr.,   57,   1673–1688,
578   10.4319/lo.2012.57.6.1673, 2012.

579   Park, J. -H., Chang, K. -I., and Nam, S.: Summertime coastal current reversal opposing offshore forcing and local
580   wind near the middle east coast of Korea: Observation and dynamics, Geophys. Res. Lett., 43, 7097–7105,
581   10.1002/2016gl069322, 2016.

582   Park, J.-H and Nam, S.: ~~Interannual variability~~Causes of ~~a surface~~interannual variation of summer mean
583   alongshore current near the ~~mid-latitude western boundary: A summer case on the Korean~~ east coast~~, Jounal~~
584   ~~of Geophysical. Research: Oceans~~ of Korea derived from 16-year long observational data, J. Geophys. Res.,
585   2018 (in revision).

586   Reifel, K. M., Corcoran, A. A., Cash, C., Shipe, R., and Jones, B. H.: Effects of a surfacing effluent plume on a
587   coastal phytoplankton community, Cont. Shelf Res., 60, 38–50, 10.1016/j.csr.2013.04.012, 2013.

588   Ryu, J. -H., Han, H. -J., Cho, S., Park, Y. -J., and Ahn, Y. -H.: Overview of geostationary ocean color imager

589   (GOCI) and GOCI data processing system (GDPS), Ocean Sci. J., 47, 223–233, 10.1007/s12601-012-0024-
590   4, 2012.

591   Son, Y. T., Chang, K. I., Yoon, S. T., Rho, T., Kwak, J. H., Kang, C. K., and Kim, K. R.: A newly observed physical
592   cause of the onset of the subsurface spring phytoplankton bloom in the southwestern East Sea/Sea of Japan,
593   Biogeosci., 11, 1319–1329, 10.5194/bg-11-1319-2014, 2014.

594   Warrick, J. A., DiGiacomo, P. M., Weisberg, S. B., Nezlin, N. P., Mengel, M., Jones, B. H., Ohlmann, J. C.,
595   Washburn, L., Terrill, E. J., and Farnsworth, K. L.: River plume patterns and dynamics within the Southern
596   California Bight, Cont. Shelf Res., 27, 2427–2448, 10.1016/j.csr.2007.06.015, 2007.

597   Yin, K. D., Zhang, J. L., Qian, P. Y., Jian, W. J., Huang, L. M., Chen, J. F., and Wu, M. C. S.: Effect of wind events
598   on phytoplankton blooms in the Pearl River estuary during summer, Cont.Shelf Res., 24, 1909–1923,
599   10.1016/j.csr.2004.06.015, 2004.

600   Yoo, S., and Kim, H. C.: Suppression and enhancement of the spring bloom in the southwestern East Sea/Japan
601   Sea, Deep-Sea Res. Pt. Ii., 51, 1093–1111, 10.1016/j.dsr2.2003.10.008, 2004.

602

603 Table 1. Sea surface temperature (SST) in °C, sea surface salinity (SSS) in g/kg, chlorophyll-a fluorescence (CF)
604 in µg/l, duration in days, and euphotic depth (Z_{eu}) in m during the E01–E10 observed from the surface mooring
605

606

		SST	SSS	CF (start & end dates)	Duration	Z_{eu}
	E01	20.5	31.2	1.65 (Jul 21–25)	4.9	Not available
2011	E02	22.3	30.9	1.91 (Jul 26–Aug 03)	8.3	Not available
	E03	24.3	29.9	1.61 (Aug 05–08.)	2.5	Not available
	E04	21.4	32.9	1.67 (Jul 16–20)	3.5	22
2012	E05	22.8	32.8	1.29 (Jul 21–27)	5.8	20.6
	E06	18.1	33.4	2.35 (Aug 29–Sep 05)	6.4	16.8
	E07	16.1	34.1	1.6 (Jul 01–04)	2.3	17.8
	E08	21.2	33.2	1.6 (Jul 12–16)	4.4	15.7
2013	E09	25.0	32.1	1.7 (Jul 28–Aug 01)	4.3	12.7
	E10	26.7	31.9	1.4 Aug 18–23)	5.9	15.2

607

608
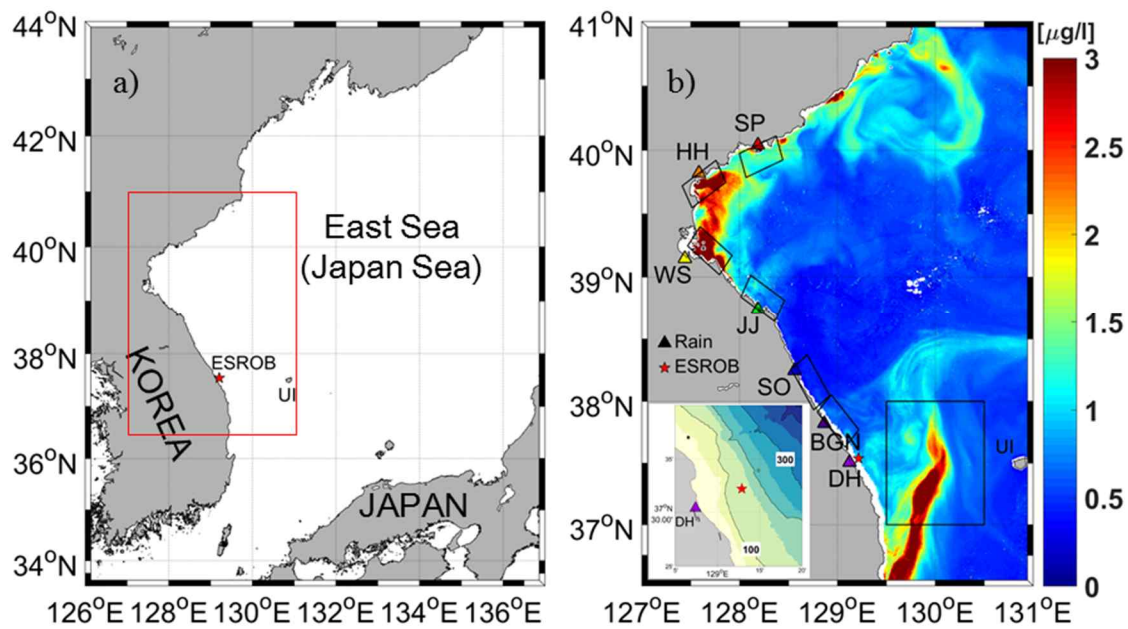
Figure 1. a) Study area in the western East Sea (Japan Sea). b) A chlorophyll a (Chl a) image from the geostationary ocean color satellite on September 6, 2012 in the area marked by red box in a). Black solid boxes denote the areas where the Chl a and TSS are averaged. Locations of the rainfall ~~station~~stations along the east coast of Korea are marked by triangles (SP: SinPho, HH: HamHeung, WS: WonSan, JJ: JangJun, SO: Sockcho, BGN: BukGangNeung, DH: DongHae, rainbow colored). The surface mooring (ESROB) is indicated by a red star in b) with bottom topography in the lower left corner where numbers denote water depth in meters (contour interval: 100 m). Ulleung Island (UI) is located at ~131 °E.

616

617

618

619
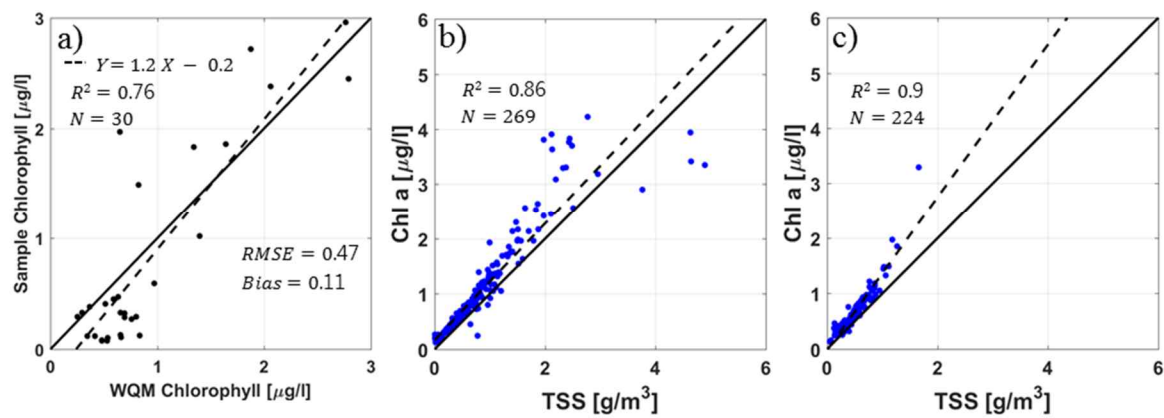
Figure 2. Results of cross-correlation (R^2: correlation coefficient) and linear regression analyses (~~dash~~dashed lines) between a) chlorophyll fluorescence measured by the ESROB WQM and absolute chlorophyll concentration obtained from in-situ water samples; and between TSS and GOCI chlorophyll a concentration for b) the areas along and near the east coast of Korea and c) area off the coast between DH and UI. The water samples (N: sample number) were collected in July and October 2011 and April 2012.
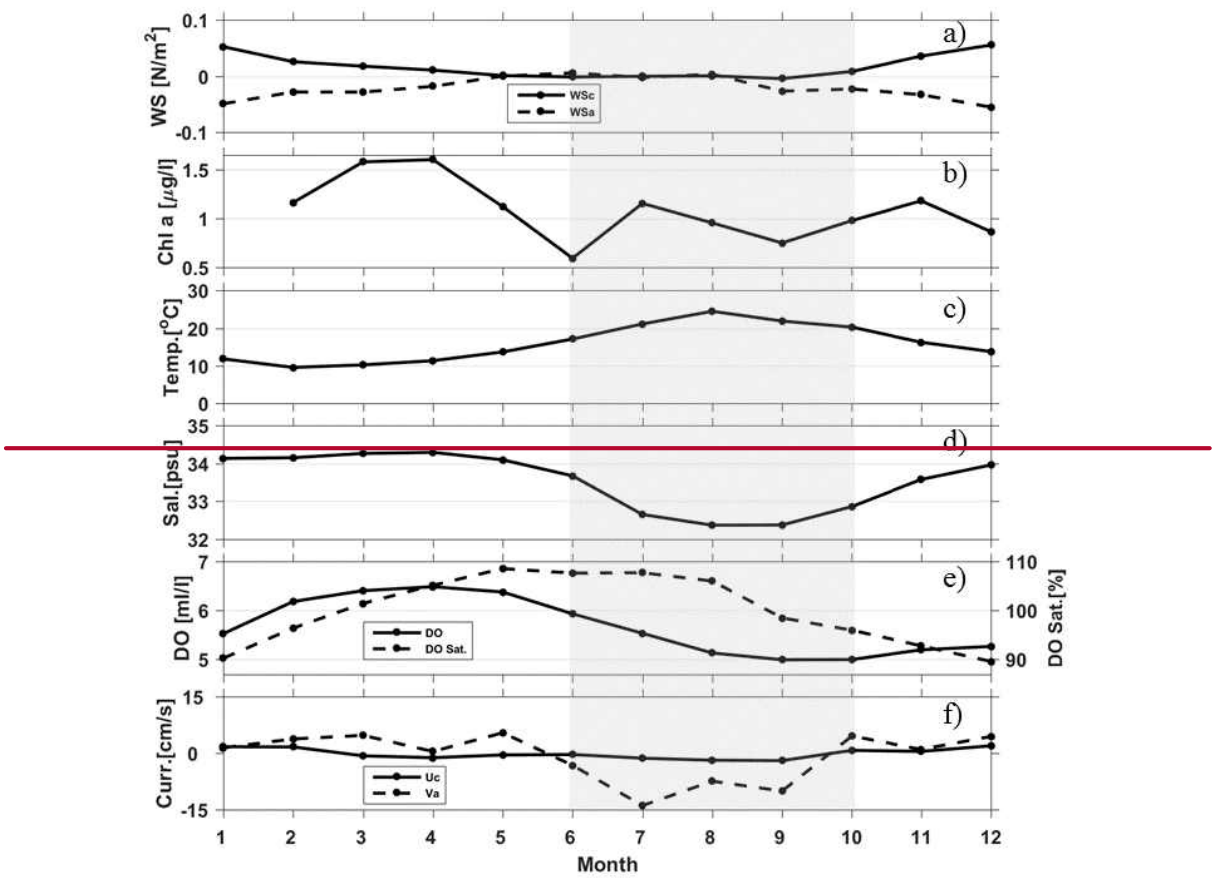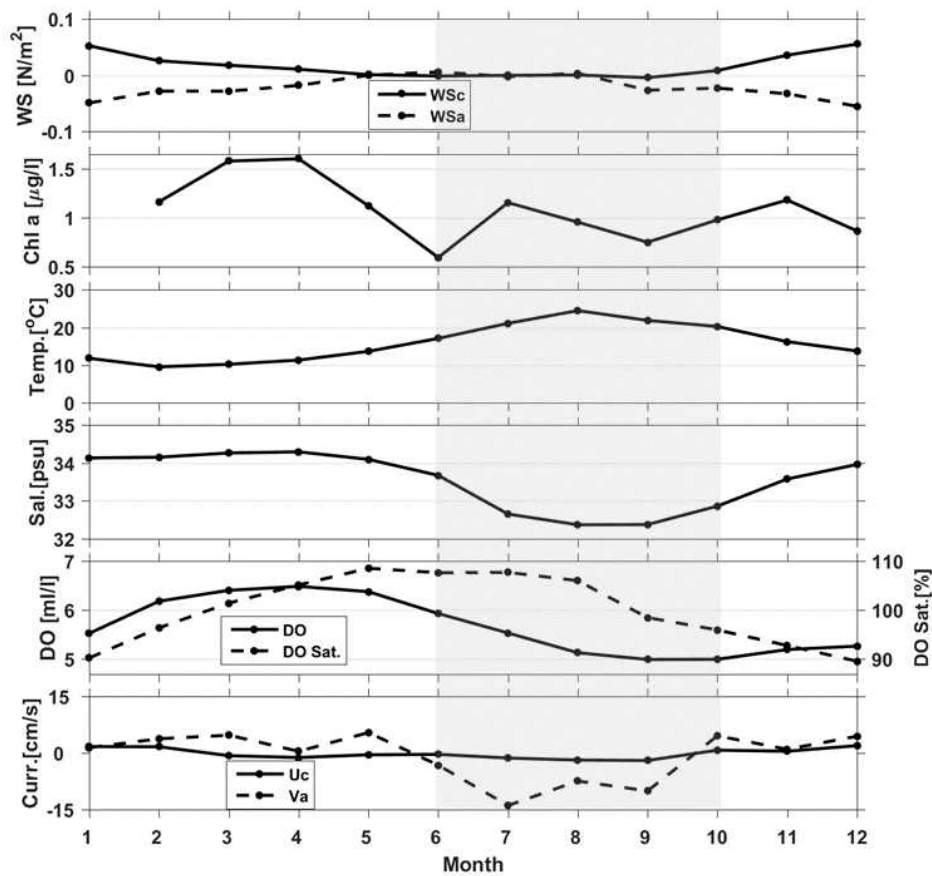
Figure 3. Climatology for a) alongshore and cross-shore components of wind stress, b) chlorophyll fluorescence, c) water temperature, d) salinity, e) dissolved oxygen in both ml/l and ~~percentage~~percent saturation, and f) alongshore and cross-shore components of surface (~ 5 m) current constructed using ESROB data collected in three years from 2011 to 2013. Summer season (JJAS) is shaded.
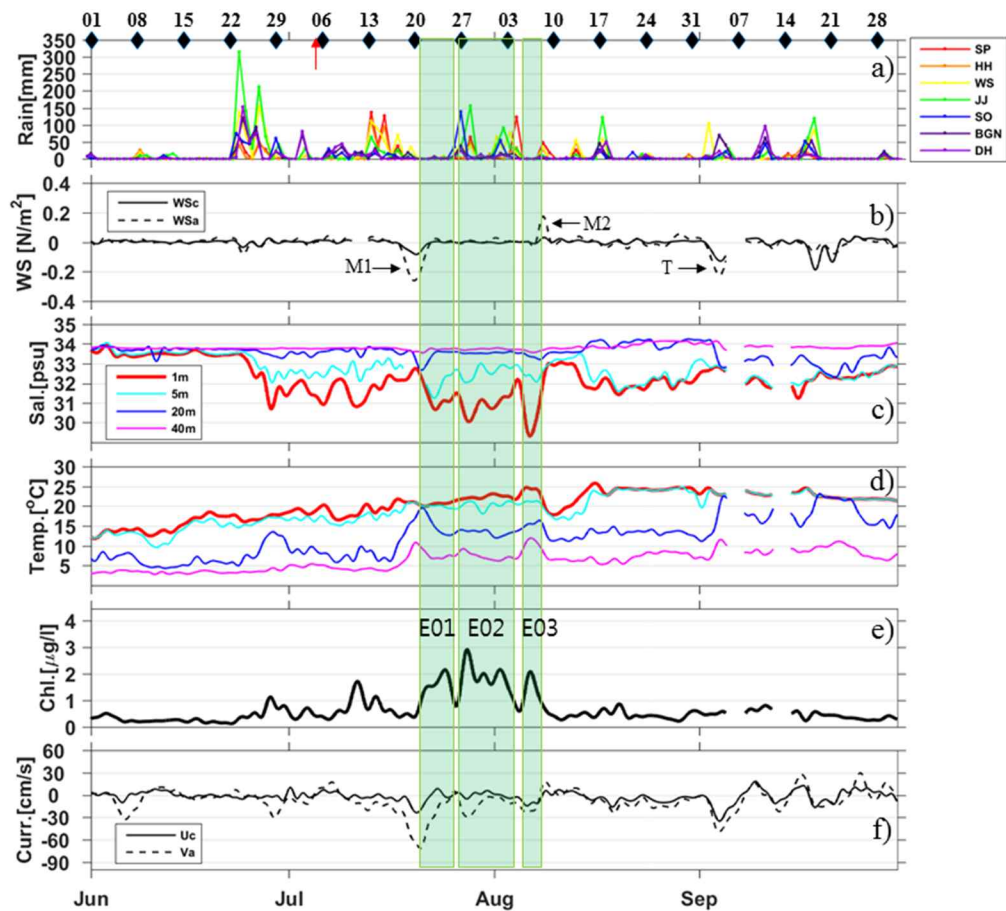
635
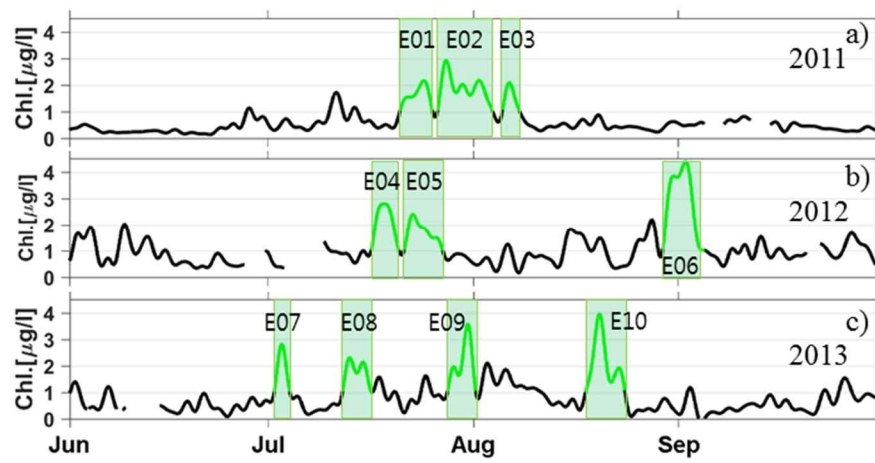
636

637   Figure 4. Time-series of low-pass filtered (cutoff period of 40 h) chlorophyll fluorescence observed at ESROB

638   during the three summers (JJAS) of a) 2011, b) 2012, and c) 2013. The episodic bloom events are green-shaded

639   and labeled E01 to E10.

640

641

642

643

Figure 5. Time-series data collected in 2011 of a) daily rainfall amounts observed at weather stations (SP: SinPho, HH: HamHeung, WS: WonSan, JJ: JangJun, SO: Sockcho, BGN: BukGangNeung, DH: DongHae) along the east coast of Korea, and b) alongshore (solid) and cross-shore (dash) wind stresses, c) salinities, and d) water temperatures observed at the surface (red), 5 (cyan), 20 (blue), and 40 m (pink), e) surface CF, and f) alongshore (dashed) and cross-shore (solid) currents, observed at ESROB. The bloom events are labeled by E01 to E03. In the top axis of (a), dates/times of satellite altimetry-derived surface geostrophic current map and geostationary satellite ocean color image (GOCI) are remarked with black diamonds and red arrow, respectively. Nearby passages of typhoons are indicated by black arrows in b) (M1: MAON, M2: MUIFA and T: TALAS).
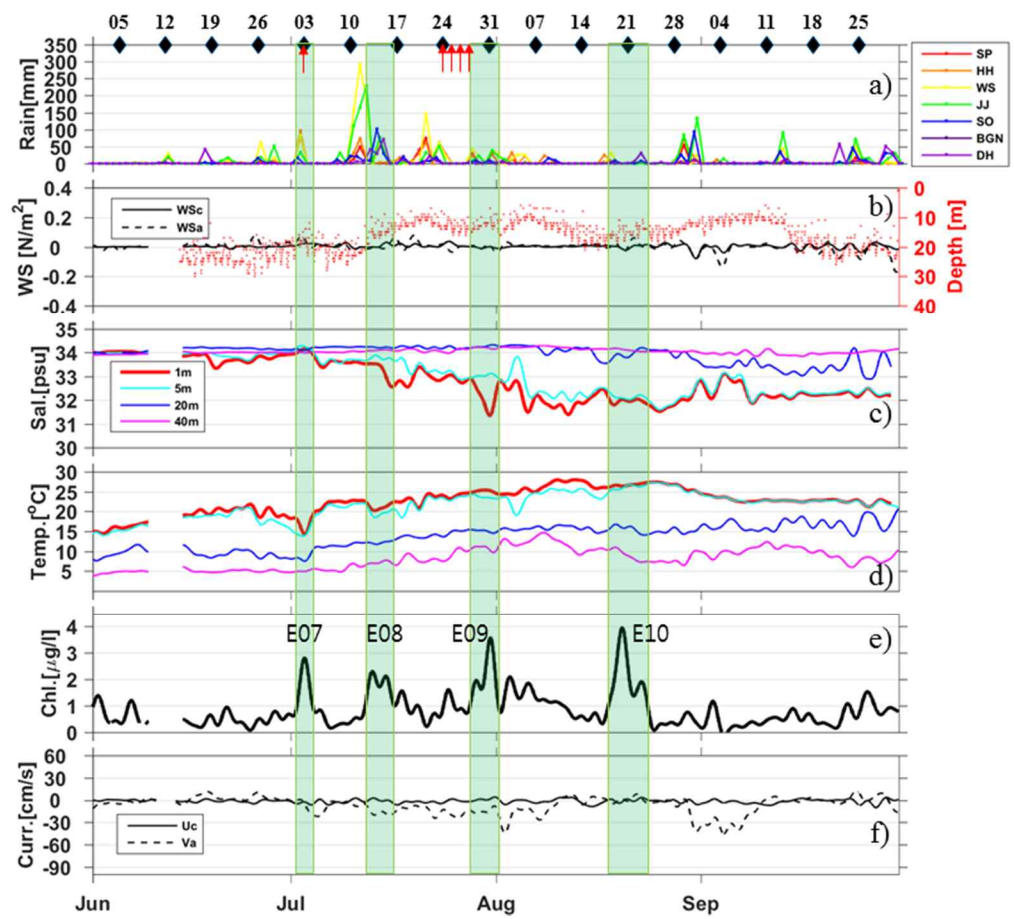
652

653

654

655

656
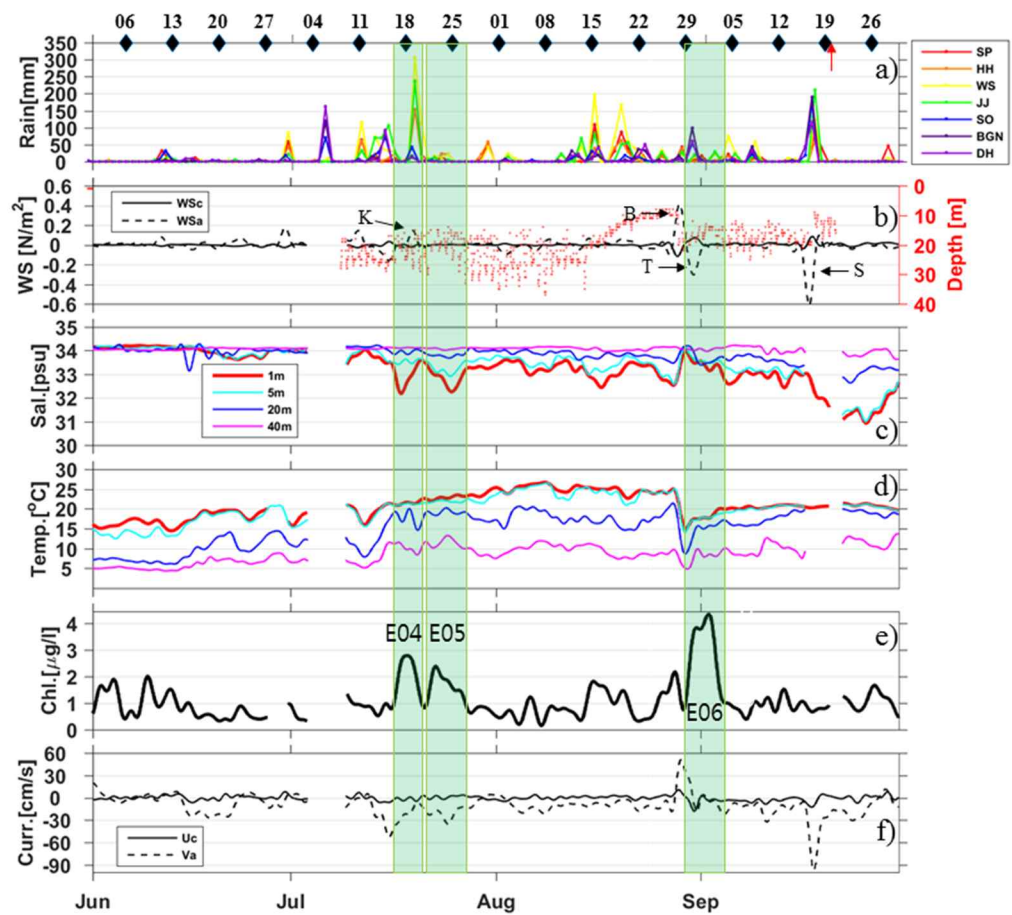
Figure 6. Same as Figure 5, but for the 2012 bloom events labeled E04 to E06, and four typhoons (K: KHANUN,
T: TENBIN, B: BOLAVEN, S: SANBA). Euphotic depth (Z_{eu}, red dots) derived from two PAR sensors attached
to the ESROB are superimposed in b).

660
661

662

663

664   Figure 7. Same as Figure 6 but for the 2013 bloom events labeled E07 to E10, and no typhoon occurrence.
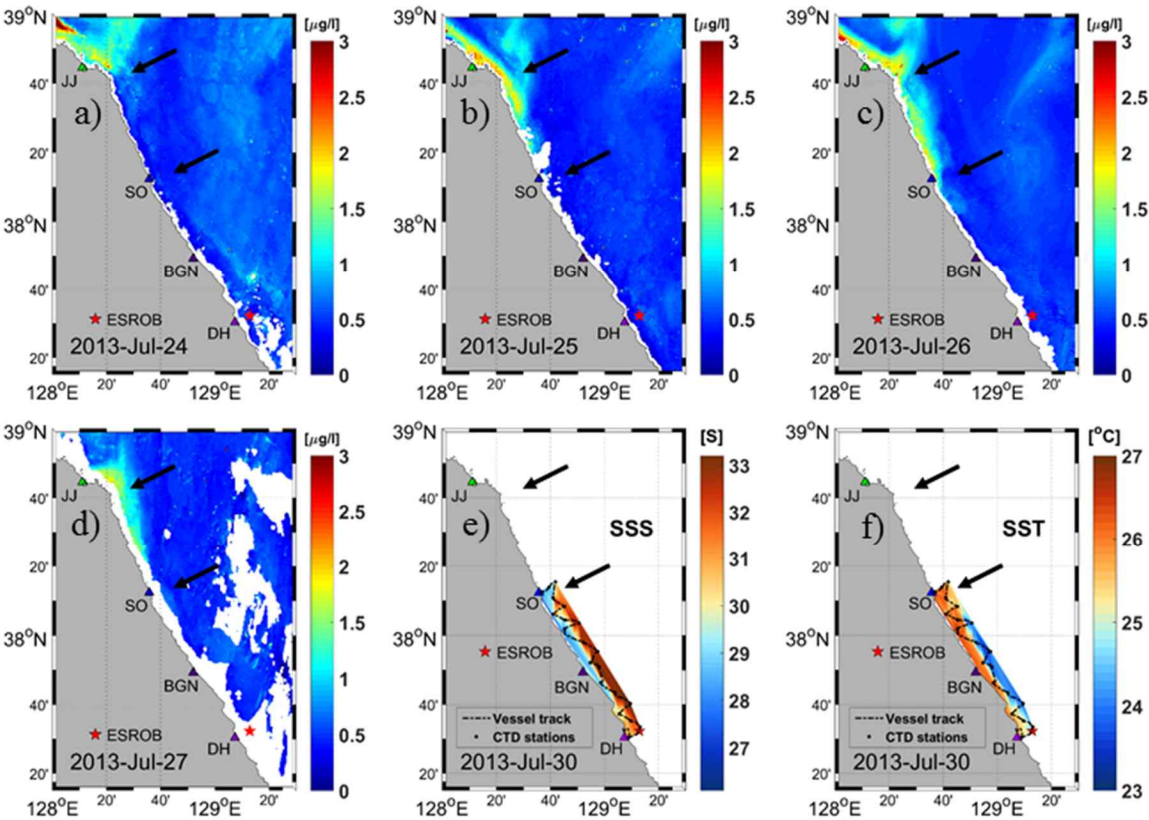
665

666

Figure 8. a)–d) Daily series of GOCI indicating surface chlorophyll a distributions from July 24 to 27, 2013. Surface distributions of in-situ e) salinity and f) temperature (dashed lines: ship tracks; dots: CTD stations) in July 30, 2013 a couple of days after heavy rainfall in the region. Two black arrows in each panel head for the same locations in the vicinity of JJ (JangJun) and SO (Sockcho).

676

677
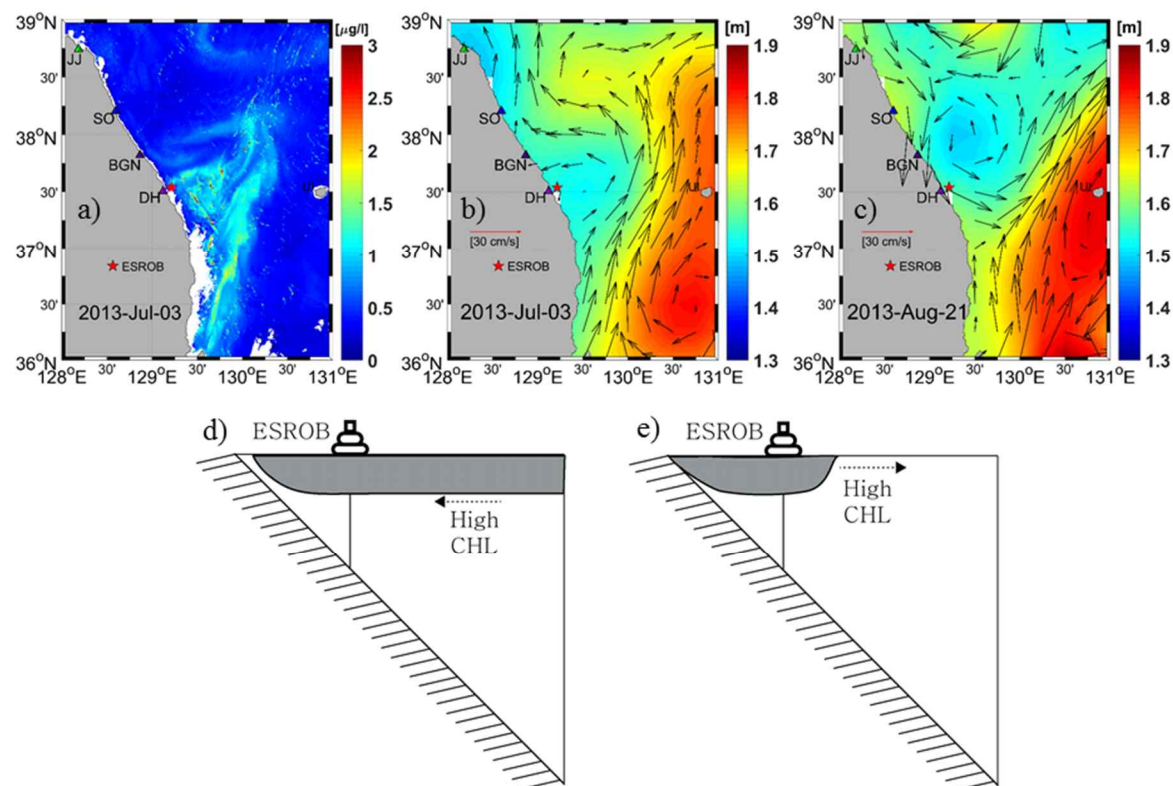
Figure 9. Distributions of a) daily composite of chlorophyll a concentration in July 3, 2013, obtained from the GOCI, and satellite altimetry-derived surface geostrophic currents in b) July 3 and c) August 21, 2013. Schematics for (d) on-shore and (e) off-shore advections of high CF surface water for July 3 (E07) and August 21 (E10), 2013.

681

682

683
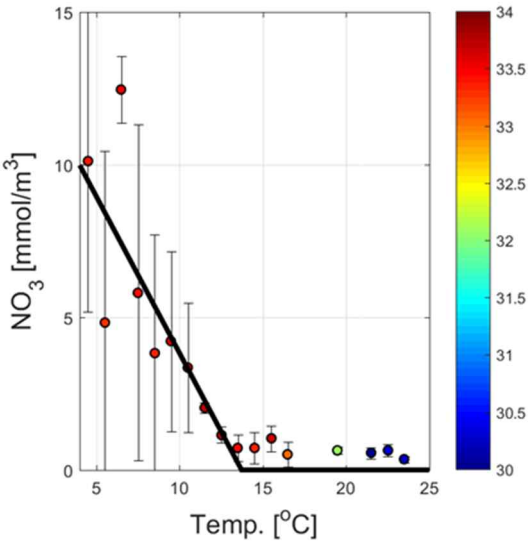
684

685   Figure 10. A linear fit (bold line) between temperature (Temp.) and nitrate (NO_3) for Temp < 14.0 °C ($NO_3 = 0$ for

686   Temp > 14.0 °C) to observations near the east coast of Korea in the summers of 2011 and 2012. Standard

687   deviations for nitrate and absolute salinity in g/kg are shown with vertical bars and colors (colorbar ~~in~~on the right),

688   respectively.

689

690
691